AMERICAN MUSEUM NOVITATES

Number 4007, 19 pp. January 23, 2024

A New Species of *Cyphocharax* Fowler (Teleostei: Curimatidae) from the Rio Xingu, Brazil

ANDRE L. NETTO-FERREIRA,[1] ACACIO F. NOGUEIRA,[2] BRUNO F. MELO,[3] AND GUILHERME M. DUTRA[4]

ABSTRACT

A new species of the curimatid genus *Cyphocharax* is described from the Rio Xingu, Amazon basin. This species is readily distinguished from congeners by the presence of a dark, round blotch on the caudal peduncle and by the high density of iridophores on the ventrolateral portion of the body, resulting in a strongly countershaded pattern. Molecular phylogenetic analyses support the recognition of the new species and suggest that it is nested within the *Curimatella alburna* clade. Ancestral state reconstruction suggests independent evolutionary origins of the blotched caudal peduncle and the countershaded ventrolateral flanks among curimatid fishes.

INTRODUCTION

The curimatid genus *Cyphocharax* Fowler (1906) includes 47 species that are broadly distributed across the Neotropics, from rivers draining the Pacific slope of southern Costa Rica to estuarine rivers and lagoons of the lower Río de La Plata drainage in northeastern Argentina (Vari, 1992a; Vari, 2003; Fricke et al., 2023). The diversity of the genus currently places it as the seventh richest within the Characiformes, and the 15th species-rich genus in the Amazon basin (Dagosta and de Pinna, 2019), with more than 20 known species of *Cyphocharax*, several of which have been formally described over the past few decades (Vari, 1992a; Vari and Black-

[1] Universidade Federal do Rio Grande do Sul, Departamento de Zoologia, Porto Alegre, Brazil.
[2] Instituto Tecnológico Vale, Desenvolvimento Sustentável, Belém, Brazil.
[3] Department of Ichthyology, American Museum of Natural History, New York.
[4] Universidade do Estado de Minas Gerais, Passos, Brazil.

 ISSN 0003-0082

ledge, 1996; Vari and Chang, 2006; Vari et al., 2012; Wosiacki and Miranda, 2013; Melo and Vari, 2014; Melo, 2017; Bortolo et al., 2018; Bortolo and Lima, 2020). The discovery and subsequent descriptions of new species of *Cyphocharax* are particularly correlated with the substantial increase of sampling efforts in many Amazonian regions, and the continuous reexamination of various species complexes within the Curimatidae (Melo et al., 2016; Melo and Oliveira, 2017), such as the *Cyphocharax spilurus* clade (Melo et al., 2018).

Recent employment of integrative taxonomy strategies combining molecular and morphological data to resolve cryptic species has become increasingly significant in describing new species of Curimatidae (Melo et al., 2016), especially in *Cyphocharax* (Melo et al., 2018, 2022; Dutra et al., 2022) and representatives of other characiform families (Agudelo-Zamora et al., 2020; Mateussi et al., 2020). That trend is continued herein with the description of a new species with a striking silvery coloration, discovered among samples of *Cyphocharax* from the Rio Xingu, a clearwater tributary of the lower Rio Amazonas in northern Brazil. The new species is herein assigned to *Cyphocharax* based on the new molecular evidence from paratypes, the lack of synapomorphies supporting its allocation on any of the other seven genera (Vari, 1989a), and the current state of knowledge on the systematics of the Curimatidae (Melo et al., 2016, 2018, 2022; Dutra et al., 2022).

MATERIALS AND METHODS

Morphological Analysis: All measurements were taken point to point to the nearest 0.1 mm with digital calipers under a stereomicroscope, preferably on the left side of specimens. Measurements and counts follow Vari (1992a) and Melo and Vari (2014). Nontype specimens were not considered paratypes for presenting any sort of damage prior or posterior to fixation. Parentheses indicate frequencies of each count, and asterisks indicate counts for the holotype. Osteological characters were examined with aid of digital radiographs and cleared and counterstained specimens, according to Taylor and Van Dyke (1985). Vertebrae of the Weberian apparatus were counted as four precaudal elements, and the fused PU1+U1 was considered a single centrum. Abbreviations used in the text are: CS = cleared and counterstained; SL = standard length. Institutional abbreviations follow Sabaj (2022). Information from the literature was also used for comparisons (Vari, 1992a; Vari and Blackledge, 1996; Vari and Chang, 2006; Vari et al., 2010, 2012). Morphometric ranges used for comparison with other *Cyphocharax* species were obtained from Vari (1992a) and subsequent taxonomic contributions on the genus.

Molecular Analyses: The phylogenetic analyses employed an expanded version of the multilocus matrix with six genes of the family Curimatidae (Melo et al., 2018), supplemented by additional taxa described recently (Melo, 2017; Melo et al., 2022; Dutra et al., 2022). In addition to the samples examined by these authors, six individuals of the new species were added to the dataset, from the Rio Culuene on the upper Xingu basin (LBP 15950) and in the middle Rio Xingu at São Felix do Xingu, Pará (LBP 17690). To maximize genetic comparisons of phenotypically similar species, two *Cyphocharax spiluropsis* from Rio Juruá (LBP 4089) and two from Rio Acre/Purus (LBP 10643), and two *Cy. gouldingi* from Rio Amapá (LBP 21189) were also added to the present analysis (table 1).

TABLE 1. Tissue samples of *Cyphocharax albiventris*, *Cy. gouldingi*, and *Cy. spiluropsis* used in this study.

Species	Voucher	Tissue number	GenBank Accession number (COI)	Locality
Cy. albiventris	LBP 15950	65710	OR807210	Rio Culuene, Canarana-MT
Cy. albiventris	LBP 15950	65711	OR807212	Rio Culuene, Canarana-MT
Cy. albiventris	LBP 15950	65712	OR807213	Rio Culuene, Canarana-MT
Cy. albiventris	LBP 17690	70478	OR807214	Rio Xingu, São Félix do Xingu-PA
Cy. albiventris	LBP 17690	70479	OR807215	Rio Xingu, São Félix do Xingu-PA
Cy. albiventris	LBP 17690	70480	OR807211	Rio Xingu, São Félix do Xingu-PA
Cy. gouldingi	LBP 21189	83104	OR807216	Rio Amapá, Amapá-AP
Cy. gouldingi	LBP 21189	83105	OR807217	Rio Amapá, Amapá-AP
Cy. spiluropsis	LBP 4089	23522	OR807218	Rio Juruá, Mâncio Lima-AC
Cy. spiluropsis	LBP 4089	23523	OR807219	Rio Juruá, Mâncio Lima-AC
Cy. spiluropsis	LBP 10643	49449	OR807220	Rio Acre, Rio Branco-AC
Cy. spiluropsis	LBP 10643	49450	OR807221	Rio Acre, Rio Branco-AC

Genomic DNA from newly sequenced specimens was extracted from muscle or fin tissues preserved in 95% ethanol using the DNeasy Tissue Kit (Qiagen Inc.). We amplified the mitochondrial protein-coding gene cytochrome *c* oxidase subunit I (COI) using the primers L6252-Asn and H7271-COXI designed for characiforms (Melo et al., 2011). PCR reactions used a volume of 12.5 µl with 9.075 µl of double-distilled water, 1.25 µl 5X buffer, 0.375 µl MgCl2 (50 mM), 0.25 µl dNTP mix, 0.25 µl of each primer at 10 µM, 0.05 µl PHT DNA polymerase enzyme (Phoneutria, Belo Horizonte, Brazil), and 1.0 µl genomic DNA (10–50 ng). The PCR program consisted of an initial denaturation (4 min at 95° C) followed by 30 cycles of chain denaturation (30 sec at 95° C), primer hybridization (30–60 sec at 52° C), and nucleotide extension (45 sec at 72° C). PCR products were seen on a 1% agarose gel and employed with dye terminators for the sequencing procedure (BigDye Terminator v 3.1 Cycle Sequencing Ready Reaction Kit, Applied Biosystems). Samples were placed into an ABI 3130-Genetic Analyzer automated sequencer (Applied Biosystems) at the Instituto de Biociências da Universidade Estadual Paulista, Botucatu, Brazil.

Sequences were assembled and edited in Geneious v7.1.9 (Kearse et al., 2012) and aligned using MUSCLE (Edgar, 2004) under default parameters. The best-fitting model of nucleotide evolution was obtained in MEGA X (Kumar et al., 2018). The phylip matrix was used to run a maximum likelihood analysis in RAxML v8.2.12 (Stamatakis, 2014) with 10 inferences on the original alignment using 10 distinct randomized maximum parsimony trees. In addition, RAxML executed 1000 nonparametric bootstrap inferences on the original alignment and stopped search with 250 ML bootstrap replicates under the MRE-based bootstopping criterion (Pattengale et al., 2010).

We performed species delimitation analyses in a submatrix containing members of the *Curimatella alburna* clade with the methods Assemble Species by Automatic Partitioning (Puillandre et al., 2021) and Poisson Tree Processes (Zhang et al., 2013). The ASAP was imple-

mented with the MUSCLE-aligned (fasta) file in the ASAP web server (https://bioinfo.mnhn.fr/abi/public/asap/) under the Kimura (k80) model with ts/tv = 2. For the PTP delimitation, the best ML tree was used as the input file in the mPTP web service (https://cme.h-its.org/exelixis/web/software/PTP/index.html) using single Poisson Tree Process with *p*-value 0.01 and *Cyphocharax vanderi* as root. Additionally, we estimated pairwise genetic distances for the submatrix in MEGA v11.0.10 (Tamura et al., 2021) using the K2P model (Kimura, 1980).

Ancestral State Reconstruction: To better understand the evolution of the pigmentation across the *Cyphocharax* sensu lato clade (Melo et al., 2018), we performed ancestral state reconstruction analyses. For the reconstruction of the caudal-peduncle blotch and the countershaded pigmentation of the flanks, those conditions were converted in binary absence vs. presence characters (table S1). The color-pattern information was obtained from examined specimens, as well as information obtained from the literature (Vari, 1984, 1989a, 1989b, 1989c, 1989d, 1991, 1992a, 1992b; Castro and Vari, 2004; Netto-Ferreira and Vari, 2011; Melo and Oliveira, 2017; Melo et al. 2016, 2022). Ancestral states were estimated with Mesquite v3.51 (Maddison and Maddison, 2021), using the Parsimony Ancestral States Reconstructions under Trace Character History.

RESULTS

***Cyphocharax albiventris*,** new species

urn:lsid:zoobank.org:act:D8EF2CA2-D1D3-4107-BD82-1624EE3123FD
Figure 1; table 2

Holotype: MPEG 35000, 79.9 mm SL, Rio Xingu, Altamira, Pará, Brazil, 03°13′20″S 52°12′57″W, 18 Jun 2012, R. Brito.

Paratypes: All from Brazil, Amazon basin, Rio Xingu basin: ANSP 195031 (1, 64.7 mm SL), Anapu, beach along the right bank near inlet to easternmost braid of Rio Xingu lower Volta Grande, 3°08′38″S 51°36′11″W, 29 Sep 2013, L.M. Sousa, A. Gonçalves, N.K. Lujan, D.B. Fitzgerald and P. M. Ito. ANSP 199638 (2, 59.7–103.1 mm SL), INPA 38029 (13, 57.1–93.4 mm SL), Altamira, Rio Iriri, ca. 8 km upstream from the confluence with Rio Xingu, 03°49′24″S 52°40′39″W, 9 Oct 2012, M.H. Sabaj, M. Arce, and L. Sousa. LBP 15950 (10), Mato Grosso, Canarana, Rio Culuene, 13°29′41.8″S 53°04′57.7″W, 02 Aug 2012, C. Oliveira, M. Taylor, G. Costa-Silva, J. Henriques. LBP 17690 (6), Pará, São Felix do Xingu, Rio Xingu, 06°39′32.5′′S 52°00′24.5′′W, 17 May 2013, R. Britzke, M. Martins; LIA 2314 (2, 45.3– 73.3 mm SL), São Felix Do Xingu, Serra do Pardo National Park, 05°46′42″S 52°36′53″W, 17 May 2015, A. Gonçalves, D. Silva. LIA 4061 (2, 61.3–61.6 mm SL), Altamira, right bank of Rio Xingu, 03°35′15″S, 52°20′40″W, 11 Oct 2013, Monitoring team. LIA 5296 (1, 67.5 mm SL), Altamira, Rio Xingu, 03°13′20″S 52°12′57″W, 19 Jun 2012, R. Brito. LIA 5309 (1, 59.9 mm SL), Altamira, Rio Xingu, 03°13′20″S 52°12′57″W, 23 Jun 2012, R. Brito. LIA 5328 (1, 60.2 mm SL), Altamira, same data as holotype. MCNIP 1847 (1, 78.9 mm SL) Vitória do Xingu, Jericoá, 3°24′33″S 51°44′20″W, 17 Jan 2013, Monitoring team. MPEG 26403 (1, 71.1 mm SL), São Félix do Xingu, igarapé São Sebastião, Serra do Jacaré,

06°06′46″S 51°48′43″W, 15 Jan 2013, P. Azevedo. MPEG 28893 (1, 68.1 mm SL), Vitória do Xingu, Belo Monte, ca. 03°08′13″S 51°41′04″W, 15 Jul 2012, L.M. Sousa. MPEG 29510 (1, 60.5 mm SL), MPEG 29584 (2, 66.6–72.0 mm SL), MPEG 29642 (3, 53.2–56.2 mm SL), MPEG 29648 (9, 56.5–65.9 mm SL). MPEG 29651 (4, 71.4–95.5 mm SL), Altamira, Rio Xingu, praia da Tartaruga, 03°35′03″S 52°20′30″W, 4 Jul 2012, L.M. Sousa. MPEG 29688 (1, 82.8 mm SL), Vitória do Xingu, Rio Bacajá, Pariaxá, 03°33′32″S, 51°40′30″W, 22 Sep 2012, D.A. Bastos. MPEG 29724 (7, 64.9–70.0 mm SL), Vitória do Xingu, Rio Xingu, ilha da Fazenda, 03°34′43″S 51°54′32″W, 7 Jul 2012, L.M. Sousa. MPEG 29731 (1, 68.6 mm SL), Altamira, Rio Iriri, cachoeira Grande, 03°50′37″S 52°44′07″W, 14 Sep 2012, L.M. Sousa. MPEG 29773 (1, 85.3 mm SL), Altamira, praia do Paratizinho (Cajueiro), 03°16′12.8″S 52°05′32.4″W, 18 Sep 2012, L.M. Sousa. MPEG 29931 (2, 70.9–71.1 mm SL), Vitória do Xingu, Belo Monte site, ca. 03°08′13″S 51°41′04″W, 15 Jul 2012, L.M. Sousa. MPEG 29945 (1, 73.7 mm SL), Vitória do Xingu, Igarapé Belo Monte, 03°06′46″S 51°37′42″W, 16 Jul 2012, L.M. Sousa. MPEG 34997 (4, 72.8–96.6 mm SL), MPEG 34998 (1, 75.3 mm SL), MPEG 34999 (1, 79.0 mm SL), Altamira, Levi's area, 03°35′15″S 52°20′40″W, 16 Nov 2012, Monitoring team. MPEG 35001 (1, 92.9 mm SL), MPEG 35002 (1, 96.3 mm SL), Altamira, praia da Fumaça, 03°35′05″S 52°20′34″W, 10 Jan 2013, Monitoring team. MPEG 35003 (1, 86.9 mm SL), Altamira, praia do Paratizinho (Cajueiro), 03°16′13″S 52°05′32″W, 14 Jan 2013, Monitoring Team. MPEG 35004 (2CS, 73.8–81.8 mm SL), Vitória do Xingu, praia da Mucura, 03°23′42″S 51°43′36″W, 20 Oct 2013, A. Gonçalves, T. Albuquerque, M. Mendonça.

Nontype Specimens: All from Brazil, Rio Xingu. MPEG 29583 (1, 72.0 mm SL), Altamira, ilha Grande, 03°34′43″S 52°23′41″W, 04 Jul 2012, L.M. Sousa. MPEG 29679 (1, 69.7 mm SL), Altamira, Itapuama, 03°36′57″S 52°20′53″W, 3 Jul 2012, L.M. Sousa. MPEG 29748 (2, 75.2–107.6 mm SL), Altamira, praia do Paratizinho (Cajueiro), 03°16′13″S 52°05′32″W, 18 Sep 2012, L.M. Sousa. MPEG 29794 (1, 67.5 mm SL), Vitória do Xingu, Jericoá, 03°23′59″S 51°44′09″W, 8 Jul 2012, L.M. Sousa. MPEG 35005 (3, 60.8–66.2 mm SL), Anapu, Rio Bacajá, praia Pariaxá, 03°34′28″S 51° 35′45″W, 19 Oct 2013, A. Gonçalves, J. Santos. Mato Grosso. MZUSP 89900 (10, 54.3–65.9 mm SL), Rio Culuene, Paranatinga, Mato Grosso, 13°51′19″S 53°15′15″W, 15 Jan 2006, A. Akama and J. Birindelli.

Diagnosis: *Cyphocharax albiventris* differs from congeners, except *Cy. leucostictus*, *Cy. platanus*, and *Cy. magdalenae*, by the strongly countershaded body with the epidermis on scales below the lateral line series nearly hyaline, lacking dark chromatophores, and the abundant iridophores present on the dermis, along the lateroventral portion of body, resulting in silvery reflective pigmentation (vs. dorsal and ventral portions of the flanks presenting similar pigmentation, with iridophores mostly restricted to head and base of scales). The new species can be diagnosed from *Cy. leucostictus* and *Cy. magdalenae* by the presence of a dark blotch on the caudal peduncle (vs. absence) and from *Cy. platanus* by the rounded shape of that blotch (vs. horizontally elongated blotch). *Cyphocharax albiventris* further differs from other *Cyphocharax* by the following combination of characters: (1) 33–36 pored scales from the supracleithrum to the hypural joint (vs. 4–9 in *Cy. aninha*, 29–32 in *Cy. meniscaprorus* and *Cy. oenas*, 48–54 in *Cy. platanus*); (2) five scale rows between lateral line and anal-fin origin (vs. 8–10 in *Cy. platanus*, and 6–7 in *Cy. tamuya*); (3) 16 circumpeduncular scales (vs. 20 in *Cy. naegelii*, 23–25 in

TABLE 2. Morphometric data of *Cyphocharax albiventris.* Range includes values for type specimens include the holotype. *N* = 29.

	Holotype	Range	Mean	SD
Standard length (SL; mm)	79.9	64.9–107.5	–	–
Percentages of SL				
Greatest body depth	33.8	30.6–35.8	33.1	1.1
Snout to dorsal-fin origin	47.3	46. 5–48.5	47.4	0.6
Snout to pectoral-fin origin	29.3	25.8–29.6	27.9	1.0
Snout to pelvic-fin origin	53.7	51.6–55.1	53.4	0.8
Snout to anal-fin origin	81.1	79.4–82.9	80.8	0.7
Snout to anus	77.3	73.8–77.3	76.1	0.7
Dorsal-fin origin to hypural joint	60.7	56.2–60.7	58.0	1.0
Dorsal-fin origin to anal-fin origin	48.0	43.2–48.0	45.8	1.0
Dorsal-fin origin to pelvic-fin origin	33.5	31.9–35.9	33.4	1.0
Dorsal-fin origin to pectoral-fin origin	32.8	31.1–35.9	33.4	1.1
Caudal-peduncle depth	11.9	10.8–12.5	11.9	0.4
Pectoral-fin length	17.5	16.0–18.3	17.3	0.6
Pelvic-fin length	21.0	19.4–21.9	20.3	0.5
Dorsal-fin length	27.7	26.3–28.7	27.6	0.6
Head length (HL)	28.4	26.9–28.4	28.0	0.8
Percentages of HL				
Snout length	34.6	29.8–34.6	31.9	1.2
Orbital diameter	34.9	33.4–38.5	35.9	1.3
Postorbital length	39.2	32.4–39.2	36.5	1.3
Interorbital distance	43.3	32.1–43.3	36.1	2.5

Cy. platanus, and 19–20 in *Cy. tamuya*); (4) nine branched rays on dorsal fin (vs. 10–12 in *Cy. spilotus*); (5) 31–32 total vertebrae (vs. 29–30 in *Cy. aninha*, 33 in *Cy. tamuya*, and 34 in *Cy. naegelii*); (6) absence of a fleshy expansion of the upper lip overlapping lower jaw (vs. upper lip very fleshy and overlapping lower jaw in *Cy. mestomyllon*); (7) lower body depth (30.6%–35.8% of SL vs. 36%–45% in *Cy. gillii*, and 38%–42% of SL in *Cy. gouldingi*); (8) shorter head length (26.9%–29.6% of SL vs. 32%–36% of SL in *Cy. oenas*); (9) lower caudal peduncle depth (10.9%–12.5% of SL vs. 14%–15% of SL in *Cy. oenas*); and (10) slightly shorter pelvic-fin length (19.4%–21.9% SL vs. 22%–27% in *Cy. spiluropsis*).

Description: Morphometric data are presented in table 2. Body somewhat elongate. Greatest body depth at vertical through dorsal-fin origin. Dorsal profile of head strongly convex from margin of upper lip to vertical through anterior nostril, slightly concave to nearly straight from that point to supraoccipital spine. Dorsal profile of body convex from tip of supraoccipital spine to dorsal-fin terminus; slightly convex from that point to adipose-fin origin and then slightly concave to origin of caudal-fin upper lobe. Ventral profile of body convex from lower lip to rear of anal fin; concave

from that point to origin of anteriormost ventral caudal-fin procurrent ray. Prepelvic region smoothly flattened transversely. Postpelvic region of body transversely rounded.

Head compressed, pointed overall in lateral view. Mouth subterminal, located at horizontal through ventral margin of orbit. Upper jaw slightly longer than lower jaw. Nostrils close together and separated by thin flap of skin. Anterior nostril circular, near midpoint between snout tip and anterior margin of eye. Posterior nostril crescent shaped. Adipose eyelid more developed anteriorly, with vertically ovoid opening near center of eye. Eye on anterior one-half of head length. Branchial membranes joined at isthmus. Branchiostegal rays 4(2).

Scales cycloid. Lateral-line pored scales from supracleithrum to hypural joint 33*(5), 34(24), 35(20) or 36(2), pores forming a straight laterosensory canal. Pored scales posterior to hypural joint 2(27) or 3*(24). Scales in transverse series from dorsal-fin origin to lateral line 5*(31). Scales in transverse series from anal-fin origin to lateral line 5*(31). Scales between anus and anal-fin origin 1(3), 2*(27) or 3*(1). Middorsal series of scales from rear of supraoccipital spine to dorsal-fin origin 10(2) or 11*(29). Circumpeduncular scales 16*(31). Scales covering basal portion of caudal-fin rays distinctly smaller than those on posterior portion of caudal peduncle.

Pectoral fin pointed, with i,13(1), i,14(8), i,15*(19), or i,16(3) rays; tip of adpressed pectoral fin reaching vertical through eighth lateral line scale. Supraneurals 4(3) anterior to neural spine of fifth to eighth vertebrae. Dorsal fin pointed, with ii,9*(31) rays; first unbranched ray about one-half length of second unbranched ray, second unbranched and first branched rays longest; branched rays gradually decreasing in size posteriorly. Dorsal-fin pterygiophores 11*(3); first inserted immediately posterior to neural spine of vertebra 8(1) or 9(2). Pelvic fin emarginate, with i,8*(31) rays; fin origin at vertical through third or fourth branched dorsal-fin ray. Tip of adpressed pelvic fin falling short of anus by one or two scales. Anal fin emarginate, with ii,7*(31) rays; first unbranched ray about one-third length of second unbranched ray; second unbranched ray and first branched rays longer, subsequent branched rays gradually decreasing in size. Anal-fin pterygiophores 8(1) or 9(2); first inserted immediately posterior to haemal spine of vertebra 20(2) or 21(1) vertebrae. Adipose fin present. Caudal fin forked with lobes somewhat pointed, i,9/8,i*(11) rays. Dorsal caudal-fin procurrent rays 7(3); ventral caudal-fin procurrent rays 5(1) or 6(2). Total vertebrae 31(1) or 32(2). Precaudal vertebrae 20(3), caudal vertebrae 11(1) or 12(2).

Coloration in Alcohol: Overall coloration retaining guanine on scales silvery (fig. 1). Background coloration of body tan. Dark coloration on dorsal portion of head, maxilla, upper lip, and infraorbital 1 lighter ventrally. Dark chromatophores on postorbital region of head slightly larger than those on snout. Overall pigmentation of latter portion of postorbital region consequently lighter than adjoining areas. Body strongly countershaded with integument on dorsum distinctly darker than skin on ventral portion of body, retaining abundant iridophores, resulting in silvery reflective pigmentation; specimens underwent extended periods in formalin showing distinctive contrast between dorsal and ventral portions of flanks, due to lack of distinct melanophores. Scale rows above lateral line series with dark chromatophores concentrated near focus of each scale. Scales below lateral line almost hyaline, lacking dark chromatophores. Dark, round

FIG. 1. *Cyphocharax albiventris*, MPEG 35000, holotype, 79.9 mm SL, Brazil, Pará, Altamira, Rio Xingu.

blotch onto midlateral scales and proximal portions of median caudal-fin rays. Distal portions of dorsal fin scattered by discrete, dark chromatophores. Distal border of adipose fin outlined by small, dark chromatophores. Pectoral, pelvic, and anal fins hyaline overall.

Distribution: *Cyphocharax albiventris* is widely distributed along the Rio Xingu basin from Rio Culuene to downstream Volta Grande and Belo Monte Dam (fig. 2). The apparent disjunct distribution seems to be due to sampling gaps in protected areas such as indigenous territories and national parks and forests.

Etymology: The specific epithet *albiventris* is formed from the combination of Latin *albus*, "white," and *venter*, "belly." It refers to the strong deposition of guanine between dermis and hypaxial muscles that results in a whitish coloration in the ventrolateral surface of body.

Relationships and Species Delimitation: The maximum likelihood tree (best score: -68024.096354) resultant from the expanded molecular data matrix (available in the online supplement: https://doi.org/10.5531/sd.sp.63) indicated *Cyphocharax albiventris* as a member of the *Curimatella alburna* clade (fig. 3). The statistical support for the position of the species within this group is relatively low (38%), as is recurrent at the base of all *Cyphocharax* and *Curimatella* lineages (fig. 3). The low support prevents us from suggesting taxonomic adjustments at the genus level, in the direction of recognizing only monophyletic genera, as *Cyphocharax* is currently paraphyletic, with *Curimatella* and *Steindachnerina* nested within it. Therefore, the generic classification of Vari (1991, 1992a,b) for the Curimatidae was followed herein, as it still is the current generic delimitation in usage (Fricke et al., 2023).

Within that group, the species represents a separate lineage as sister to the clade including *Curimatella alburna*, *Cyphocharax microcephalus*, *Cu. dorsalis*, *Cu. meyeri*, *Cu. immaculata*, as well as *Cy. leucostictus*, *Cy. notatus*, and *Cy. plumbeus*. Despite its close relationship with the aforementioned *Curimatella*, *Cy. albiventris* lacks scale sheets in the caudal-fin lobes, promptly distinguishing it from those species. On the other hand, those species share the strongly countershaded pigmentation pattern, which, in addition to the genetic data presented herein, suggests evidence of close

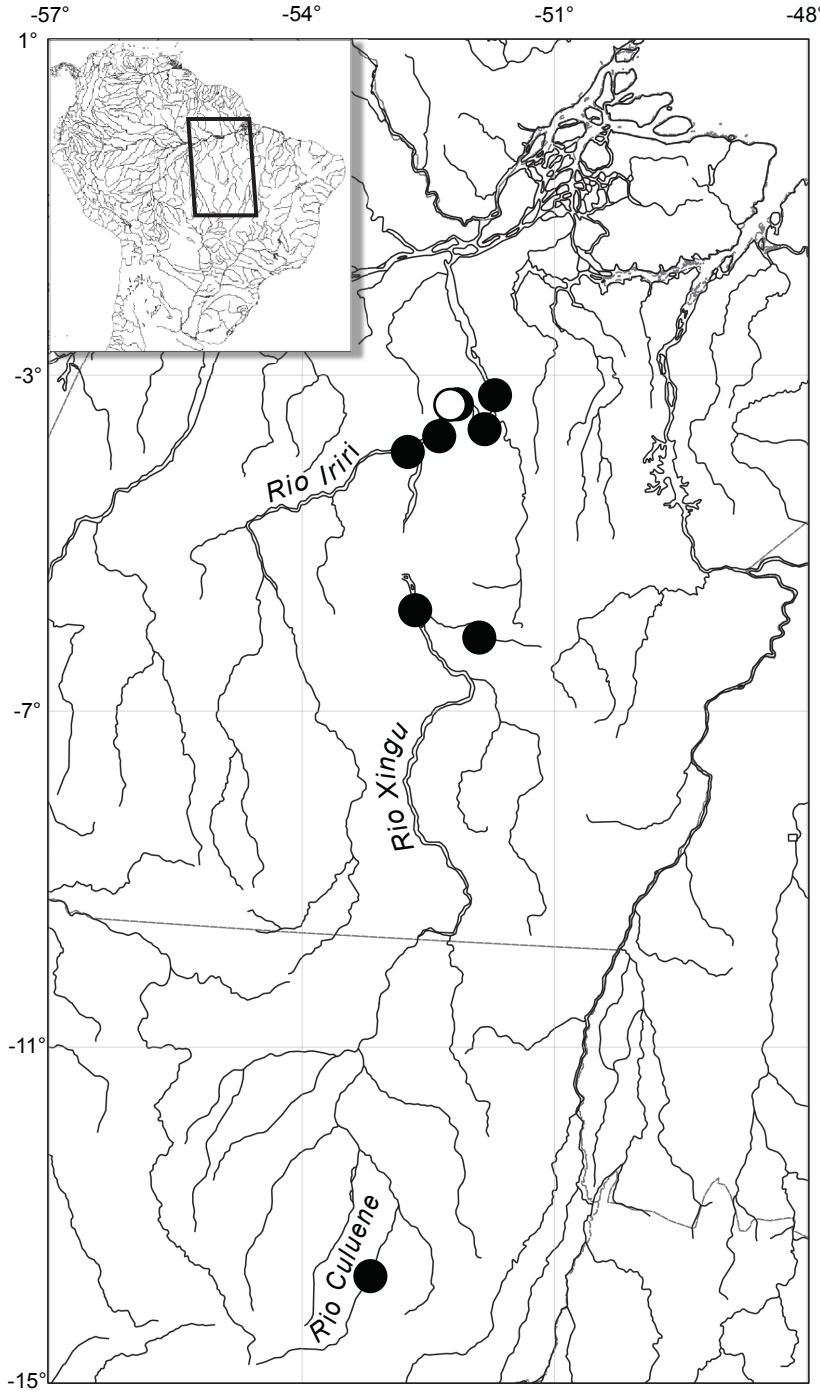

FIG. 2. Map of the Rio Xingu basin and adjoining area showing collection sites (dark circles) and the type locality (white circle) of *Cyphocharax albiventris*. Some symbols represent more than one collection site.

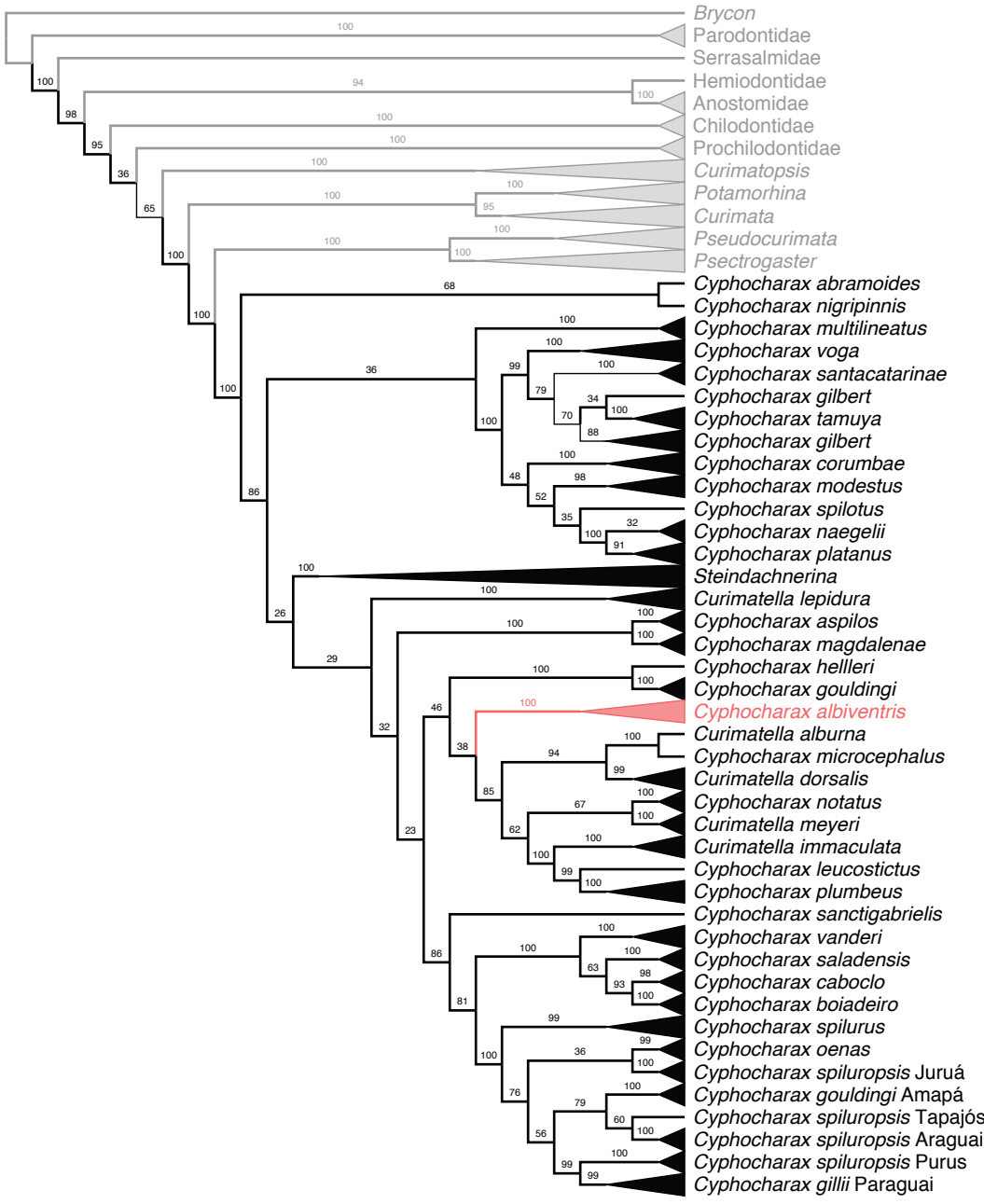

FIG. 3. Maximum-likelihood tree of the multilocus data matrix of Curimatidae highlighting the position of *Cyphocharax albiventris* within the *Curimatella alburna* clade. Numbers near nodes represent bootstrap support.

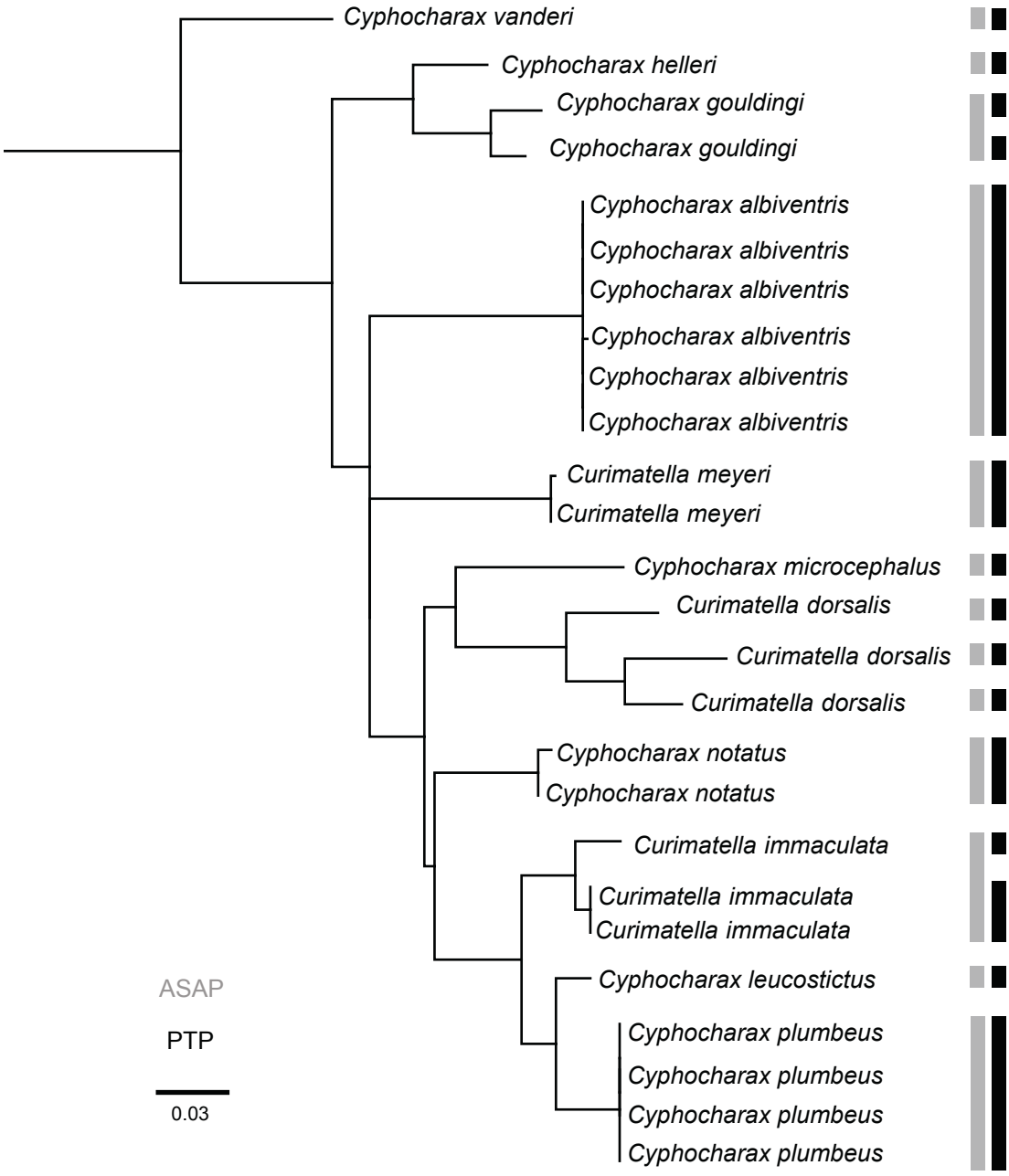

FIG. 4. Species delimitation within the *Curimatella alburna* clade recognized by the ASAP and PTP methods indicated in grey and black bars, respectively.

relationship. Among the species lacking caudal-fin scales, the new species differs from *Cy. leucostictus* and *Cy. plumbeus* by the presence of the caudal blotch onto the caudal peduncle distal tip and the proximal portions of median caudal-fin rays (vs. caudal blotch absent).

In all analyses, the monophyly of the species presented the maximum support (100%) and the lineage has an extremely long branch indicating accumulation of nucleotide substitutions and consequently high genetic distance relative to the other species of the *Curimatella alburna* clade. The best distance-based ASAP partition (ASAP score = 2, *p* value = 0.01194, threshold distance = 0.035; the lower the score, the better the partition) delimited 13 species with the six individuals attributable to *Cyphocharax albiventris* being delimited as a single Molecular Operational Taxonomic Unit or putative species (fig. 4). The PTP model delimited 15 species in total (best score for single coalescent rate: 74.829184 > null-model score: 70.702021) with the six specimens of *Cy. albiventris* assigned to a unique species as in the result of the ASAP method (fig. 4). A matrix of average intra- and interspecific K2P genetic distance for each species of the of the *Curimatella alburna* clade is shown in table 3. Values of interspecific distance for the new species ranged from 9.7% with *Cyphocharax notatus* to 13.2% with *Cu. immaculata*, whereas the intraspecific distance within the new species was 0.06%. Therefore, there is compelling molecular evidence for the recognition of that lineage as a distinct species, described herein as *Cy. albiventris*.

Ancestral State Reconstruction: The codifications for the ancestral state reconstructions of each taxon on the matrix are presented in table S1 (available in the online supplement: https://doi.org/10.5531/sd.sp.63). Despite the considerable variation in form and position, the caudal blotch was considered homologous in all taxa presenting that pigmentation element on the posterior portion of the caudal peduncle, throughout the representatives of the family. Considering the obtained phylogenetic hypothesis, the reconstruction resulted in 16 transformations, all within the Curimatidae. The dark pigmentation on the caudal peduncle originated in eight independent instances and was reversed eight times independently in the family (fig. S1). The origins occurred in *Curimatopsis* (reversed in *Curimatopsis pallida*), *Potamorhina laticeps*, *Pseudocurimata*, subclade of the *Psectrogaster ciliata* clade (reversed in *P. ciliata*), a subclade of the *Cyphocharax gilbert* clade, base of *Steindachnerina* (reversed in *S. hypostoma* clade and *S. dobula* clade), within *Curimatella alburna* clade (reversed in *Cu. alburna* and some members), and the *Cyphocharax spilurus* clade (fig. S1).

Within the Curimatidae, the strong countershading evolved in eight independent instances: *Potamorhina* and *Curimata*, *Pseudocurimata boulengeri*, *Psectrogaster*, *Cyphocharax platanus*, within the *Steindachnerina hypostoma* clade, *Curimatella lepidura*, *Cy. magdalenae*, and the base of the *Cu. alburna* clade. Three independent secondary losses occurred within the *Cu. alburna* clade: *Cy. microcephalus*, *Cy. notatus*, and *Cy. plumbeus* (see fig. S2 in the online supplement: https://doi.org/10.5531/sd.sp.63).

Comparative Material Examined: *Cyphocharax abramoides*: MPEG 23568 (4, 89.3–129.8 mm SL), Floresta Nacional Caxiuanã, Pará, Brazil. – *Cyphocharax albula*: MCNIP 807 (holotype of *Cy. lundi*, 73.7 mm SL), Rio das Velhas, Rio São Francisco, Brazil. – *Cyphocharax aninha*: MPEG 15767 (25 paratypes, 17.1–21.1 mm SL), Rio Mopeco, Rio Paru, Brazil. – *Cyphocharax aspilos*:

TABLE 3. Genetic distances among species of the of the *Curimatella alburna* clade. Interspecific distances below diagonal; standard deviation above diagonal. Bold numbers represent intraspecific genetic distances.

	1	2	3	4	5	6	7	8	9	10	11
1. *Cy. vanderi*	**n/c**	0.0163	0.0157	0.0176	0.0195	0.0180	0.0166	0.0144	0.0167	0.0170	0.0168
2. *Cu. dorsalis*	0.1355	**0.0683**	0.0143	0.0154	0.0157	0.0139	0.0149	0.0135	0.0137	0.0149	0.0143
3. *Cy. helleri*	0.1161	0.1111	–	0.0107	0.0144	0.0172	0.0160	0.0140	0.0136	0.0162	0.0152
4. *Cy. gouldingi*	0.1353	0.1290	0.0674	**0.0338**	0.0154	0.0166	0.0162	0.0149	0.0147	0.0169	0.0160
5. *Cu. meyeri*	0.1561	0.1273	0.0980	0.1151	**0.0018**	0.0144	0.0163	0.0155	0.0166	0.0168	0.0157
6. *Cy. microcephalus*	0.1412	0.1113	0.1333	0.1342	0.0944	–	0.0160	0.0138	0.0137	0.0163	0.0161
7. *Cy. albiventris*	0.1218	0.1174	0.1085	0.1225	0.1096	0.1226	**0.0006**	0.0146	0.0163	0.0168	0.0156
8. *Cy. notatus*	0.1073	0.1128	0.0980	0.1129	0.1061	0.0933	0.0970	**0.0055**	0.0127	0.0130	0.0126
9. *Cu. immaculata*	0.1225	0.1115	0.0996	0.1142	0.1250	0.1007	0.1325	0.0902	**0.0161**	0.0107	0.0101
10. *Cy. plumbeus*	0.1325	0.1115	0.1202	0.1302	0.1258	0.1171	0.1304	0.0894	0.0636	**0.0000**	0.0080
11. *Cy. leucostictus*	0.1281	0.1094	0.1070	0.1190	0.1146	0.1173	0.1154	0.0832	0.0542	0.0376	–

USNM 121311, 2 paratypes, 104.6–108.5 mm SL, Rio Palmar, Venezuela. – *Cyphocharax biocellatus*: ANSP 189146, holotype, 62.8 mm SL, Suriname, Sipaliwini, Litanie basin. – *Cyphocharax boiadeiro*: LIRP 14133 (holotype, 42.9 mm SL), Rio Araguaia, Mato Grosso, Brazil. – *Cyphocharax caboclo*: MNRJ 52506, (holotype, 59.1 mm SL), Rio Correntes, Itiquira, Brazil. – *Cyphocharax corumbae*: MZUSP 52361 (holotype of *Steindachnerina corumbae*), 109.7 mm SL, Rio Pirapitinga, Caldas Novas, Brazil. – *Cyphocharax derhami*: AMNH 274311, Rio Ucayali, Jenaro Herrera, Peru. – *Cyphocharax festivus*: USNM 280426, holotype, Peru, Loreto, caños entering Rio Nanay. MZUSP 41300 (5 paratypes, 50.3–61.4 mm SL), Río Nanay, Peru. – *Cyphocharax gangamon*: MZUSP 22037 (holotype, 48.4 mm SL), Monte Cristo, Rio Tapajós, Brazil. MZUSP 41762 (8 paratypes, 25.3–34.6 mm SL), Monte Cristo, Rio Tapajós, Brazil. – *Cyphocharax gilbert*: MCNIP 207 (1, 144.8 mm SL), Rio Corrente Grande, Rio Doce. – *Cyphocharax gillii*: LBP 10789 (16, 24.8–67.0 mm SL), Rio Paraguai, Brazil. – *Cyphocharax gouldingi*: MZUSP 41762 (holotype, 94.0 mm SL), Rio Cupixi, Amapá, Brazil. MZUSP 41763 (13 paratypes, 65.2–88.3 mm SL), Rio Cupixi, Amapá, Brazil. MZUSP 52249 (3, 42.0–50.1 mm SL), Rio Tocantins, Brazil. – INPA 47109 (9, not measured), Rio Xingu, Brazil. MPEG 12297 (4, 74.2–78.2 mm SL), Rio Urucu, Coari, Rio Solimões, Brazil. – *Cyphocharax* aff. *helleri*: INPA 3261 (15, 78.5–112.5 mm SL), Rio Trombetas, Brazil. – *Cyphocharax jagunco*: MCNIP 1612 (holotype, 48.5 mm SL), Ribeirão da Areia, Rio Jequitinhonha. – *Cyphocharax laticlavius*: USNM 336594, 9 paratypes, 24.0–30.9 mm SL, Rio Yasuni, Napo, Ecuador. – *Cyphocharax leucostictus*: MCZ 787, lectotype of *Curimatus leucostictus*, 104.3 mm SL, Brazil, Amazonas, Lago Aleixo, Rio Negro. – *Cyphocharax meniscaprorus*: USNM 235484, 13 paratypes, Venezuela, Bolívar, Rio Aro. – *Cyphocharax mestomyllon*: MZUSP 41755 (holotype, 36.0 mm SL), Rio Marauiá, Rio Negro, Brazil. *Cyphocharax microcephalus*: MCZ 785, holotype of *Curimatus microcephalus*, 104.0 mm SL, Suriname, no exact locality. – *Cyphocharax modestus*: LBP 19718 (3, 118–128.3 mm SL), Salto, Rio Tietê, Brazil. – *Cyphocharax multilineatus*: MPEG 30316 (2, 68.2–107.1 mm SL), Lago São Francisco, Juruti, Pará, Brazil. – *Cyphocharax muyrakytan*: LBP 23759, 5 paratypes, 48.1–58.9 mm SL, Brazil, Pará, Santarém, Rio Arapiuns. – *Cyphocharax naegelii*: LBP 11250 (1, 136.1 mm SL), Rio Tietê, Brazil. – *Cyphocharax nigripinnis*: MZUSP 42025 (holotype, 53.3 mm SL), Rio Xeruini, Rio Branco, Brazil. – *Cyphocharax notatus*: MPEG 12229 (2, 113.0–114.5 mm SL), Coari, Rio Solimões, Brazil. – *Cyphocharax oenas*: LBP 18659 (6, 46.3–58.3 mm SL), Meta, Río Orinoco, Venezuela. – *Cyphocharax pantostictos*: USNM 306594, holotype, 72.5 mm SL, Laguna de Jatuncocha, Napo, Ecuador. – *Cyphocharax pinnilepis*: USNM 298248, 4 paratypes, 31.2–98.5 mm SL, Rio Gongogi, Rio de Contas, Bahia, Brazil. *Cyphocharax plumbeus*: MCZ 31493, lectotype of *Curimatus plumbeus*, 94.8 mm SL, Brazil, Amazonas, Paraná do Janauari. MPEG 184 (2, 68.8–70.7) mm SL, Rio Tapajós, Itaituba, Brazil. – *Cyphocharax punctatus*: MZUSP 38998 (23 paratypes, 16.9–24.8 mm SL), Marowijne river, Suriname. – *Cyphocharax saladensis*: LBP 6034 (8, 28.1–43.0 mm SL), Rio Maquiné, Osório, Brazil. – *Cyphocharax sanctigabrielis*: MZUSP 115004 (holotype, 60.7 mm SL), Rio Negro, Brazil. – *Cyphocharax santacatarinae*: LBP 766 (1, 39.0 mm SL), Rio Marumbi, Morretes, Brazil. – *Cyphocharax signatus*: MZUSP 41757 (holotype, 33.8 mm SL), Rio Vermelho, Rio Araguaia, Brazil. – *Cyphocharax spilotus*: USNM 285194, 10 paratypes of *Curimata spilota*, 35.9–60.6 mm SL, Rio Santa Maria, Brazil. – *Cyphocharax spiluropsis*: MCZ 98961 (lectotype of *Curimatus spiluropsis*, 65.6 mm SL), Rio Içá, Solimoes, Brazil. MCZ 20216 (2

paralectotypes of *Curimatus spiluropsis*, 50.6–52.0 mm SL), Rio Icá, Solimões, Brazil. INPA 19359 (4, not measured), Rio Solimões, Brazil. INPA 25947 (9, not measured), Rio Uatumã, Brazil. INPA 26639 (20, not measured), Rio Madeira, Brazil. INPA 43485 (5, not measured), Rio Xingu, Brazil. LBP 14163 (10, not measured), Rio Tapajós, Brazil. LBP 22424 (2, 78.3–83.0 mm SL), Rio Solimões, Leticia, Colombia. MPEG 23739 (2, 59.5–68.9 mm SL), Rio Maicuru basin, Brazil. – *Cyphocharax spilurus*: INPA 9211 (10, not measured), Rio Negro, Brazil. INPA 52713 (21, not measured), Rio Takutu, Rio Branco, Brazil. LBP 15612 (4, 39.3–59.9 mm SL), Rio Takutu, Bonfim, Brazil. – *Cyphocharax stilbolepis*: MZUSP 41759 (holotype, 108.1 mm SL), Belo Monte, Rio Xingu, Brazil. – *Cyphocharax tamuya*: MZUSP 125833 (holotype, 106.8 mm SL), Rio Paraibuna, Brazil. – *Cyphocharax vanderi*: MZUSP 4325 (holotype, 42.6 mm SL), Corumbataí, Brazil. – *Cyphocharax vexillapinnus*: MZUSP 41761 (3 paratypes, 50.8–55.0 mm SL), Río Itaya, Peru. – *Cyphocharax voga*: LBP 17002 (9, 36.0–42.3 mm SL), Lagoa dos Patos, Rio Grande, Brazil.

DISCUSSION

The generic assignment of *Cyphocharax albiventris* is supported by the expanded multilocus phylogeny of the Curimatidae (fig. 3) (sensu Melo et al., 2018), and the lack of the derived characters supporting other nominal genera, such as *Curimatella* (the *Cyphocharax* sensu Vari, 1989a, 1992a). Our results also indicate that *Cy. albiventris* is a member of the *Curimatella alburna* clade (Melo et al., 2018, 2021), a group hypothesized to have undergone initial diversification between 37 and 25 million years ago (Melo et al., 2021). The position of *Cy. albiventris* as sister to a broader group of species in the clade suggests that the cladogenetic event that led to species' evolutionary origin may have occurred prior to the Miocene channelization of the Rio Amazonas (Hoorn et al., 2010; Albert et al., 2021).

The phylogeny contrasts with the phenotypic evidence, which initially suggested *Cyphocharax albiventris* belonged to a taxonomically challenging assemblage of *Cyphocharax* species sharing a dark blotch on the caudal peduncle (Vari, 1992a). The diagnostic features allowing correct identification of those species are limited and frequently overlapping (see Diagnosis), causing not only difficulties in morphological delimitation of valid species, but also hindering the recognition of new species within the genus based solely on the morphological dataset.

Using integrative taxonomy approaches in curimatids has recently aided in overcoming these obstacles (Melo et al., 2016, 2018, 2022; Dutra et al., 2022), which has not only aided in the recognition of cryptic species but also in the differentiation of phenotypically similar ones (i.e., *Cy. gouldingi* and *Cy. spiluropsis*). That was the case in this contribution, where *Cy. albiventris* was unambiguously delimited from other congeneric species by the two methods used, so assisting the description of a new species (figs. 3, 4).

Cyphocharax albiventris has been misidentified in collections as *Cy. gouldingi*, *Cy. spiluropsis*, or even *Cy. spilurus*, due to the dark blotch on the caudal peduncle, despite its most distinguishing feature: the overall lack of melanophores and the abundant distribution of iridophores, resulting in strong guanine deposition in the ventrolateral portion of the body. *Cyphocharax spilurus* is restricted to rivers draining the Guiana Shield from Venezuela to French Guyana,

the upper Rio Branco and upper Rio Negro, and probably in the upper Río Orinoco (Vari, 1992a; Sidlauskas and Vari, 2012), being, thus, absent from the Rio Xingu basin. *Cyphocharax gouldingi* was originally described from the Rio Cupixi, a tributary of the Rio Araguari, the Rio Capim, the lower Rio Tocantins and the lower Rio Xingu, including the Volta Grande (Vari, 1992a). Subsequently, specimens of *Cy. gouldingi* were collected in the Río Napo in Ecuador, significantly extending its range (Vari and Blackledge, 1996). Finally, *Cy. spiluropsis*, is widely distributed over the Amazon basin (Vari, 1992a), and occurs sympatrically with *Cy. albiventris* in the Rio Xingu. Despite the overall similarities of the three species, *Cy. albiventris* can be distinguished from *Cy. gouldingi* and *Cy. spiluropsis* based on the lack of melanophores on the epidermis and scales, plus the abundant distribution of iridophores of the ventral portion of the flanks, resulting in the strongly countershaded color pattern, which remains detectable even after guanine deposition has been removed or degraded (i.e., caused by extended periods of formalin fixation). In *Cy. gouldingi* and *Cy. spiluropsis*, in turn, the dorsal and ventral portions of flanks present somewhat similar tones of pigmentation, with the scales and/or adjacent epidermis presenting distinct melanophores, creating a more reticulate or checkered pattern as depicted by Vari (1991). In addition, even though the number of lateral line scales between the supracleithrum and the hypural joint overlaps in body depth and lateral line scales, this number can be used to distinguish *Cy. albiventris* (34 to 37) from *Cy. gouldingi* (31 to 34), as specimen examination indicates that these features overlap only in outliers.

Until recently, artificial groups of species within the genus were proposed based on the existence of a dark caudal blotch as the predominant element of color pattern (i.e., *Cyphocharax spilurus* and *Cy. gilbert* groups; Vari, 1992a). The present relationship hypothesis among representatives of *Cyphocharax*, as well as those presented by Melo et al. (2018, 2022) and Dutra et al. (2022) suggest that its relevance as a diagnostic character among the species of *Cyphocharax* should be cautiously evaluated, as the presence of the caudal blotch is a plesiomorphic condition of a major clade including the *Curimatella alburna* and the *Cy. spilurus* clades, with two independent losses within the *Cu. alburna* clade.

Cyphocharax albiventris shares a well-marked countershading with most representatives of the *Curimatella*. That condition can also be observed in *Curimata*, *Potamorhina*, *Psectrogaster*, *Pseudocurimata boulengeri*, *Steindachnerina gracilis*, *S. planiventris*, *Cy. leucostictus*, *Cy. magdalenae*, and *Cy. platanus*. This pigmentation pattern is hypothesized to reduce detectability by visually oriented predators by reducing contrast with the water body (Donohue et al., 2020), and its expression in the aforementioned groups including migratory species of Curimatidae (i.e., *Curimata*, *Potamorhina*, and *Psectrogaster*) may provide support for this hypothesis. Compared to other curimatid fishes with similar pigmentation, the countershading could reduce detection of open water swimmers, who would otherwise be more vulnerable to predation. Finally, despite its independent, homoplasious origin (fig. S1), the condition can be considered an additional synapomorphy for the clades (*Curimata* + *Potamorhina*), *Psectrogaster*, (*Steindachnerina planiventris* + *S. gracilis*), and the *Curimatella alburna* clade (being secondarily lost in *Cy. microcephalus*, *Cy. notatus*, and *Cy. plumbeus*), and autapomorphies for *Cu. lepidura*, *Cy. platanus*, *Cy. magdalenae*, and *Pseudocurimata boulengeri*.

ACKNOWLEDGMENTS

Authors thank Melanie Stiassny, Chloe Lewis, and Thomas Vigliotta (AMNH), Susan Mochel and Caleb McMahan (FMNH), Lucia Rapp Py-Daniel and Renildo Oliveira (INPA), Claudio Oliveira (LBP), Leandro Sousa and Alany Gonçalves (LIA), Flávio Bockmann, Ricardo M.C. Castro and André Esguícero (LIRP), Gilmar Santos and Tiago Pessali (MCNIP), George Lauder (MCZ), Wolmar Wosiacki and I. Maschio (MPEG), Alessio Datovo and Michel Gianetti (MZUSP), and Lynne Parenti (USNM) for the loan of specimens and curatorial assistance. Thanks to Ariel Bradley and Kayla Savage (ANSP WINS students) for preparation of radiographs of ANSP specimens. We also are thankful to Jose L.O. Birindelli, Fernando C.P. Dagosta, Brian L. Sidlauskas, and an anonymous reviewer for criticism on earlier versions of the manuscript. Authors were financially supported by the Conselho Nacional de Desenvolvimento Científico e Tecnológico (CNPq) through the Programa de Capacitação Institucional (MPEG/MCTI) (313404/2015-1 ALN-F; 300066/2016-3 GMD), Universal (404991/2018-1 BFM), Produtividade em Pesquisa (313834/2021-0); FAPESP (2011/50282-7 ALN-F; 2016/11313-8 BFM; 2018/09445–9 GMD), FAPERGS (72550.751.48979 ALN-F), NSF (DEB-1257813 iXingu Project), and AMNH Axelrod Research Curatorship (BFM). This contribution was also supported by the Diversity and Evolution of Gymnotiformes Project (FAPESP/Smithsonian proc. 2016/19075–9).

REFERENCES

Agudelo-Zamora, H.D., J. Tavera, Y.D. Murillo, and A. Ortega-Lara A. 2020. The unknown diversity of the genus *Characidium* (Characiformes: Crenuchidae) in the Chocó biogeographic region, Colombian Andes: two new species supported by morphological and molecular data. Journal of Fish Biology 97 (6): 1662–1675.

Albert, J.S., et al. 2021. Late Neogene megariver captures and the Great Amazonian biotic interchange. Global and Planetary Change 205: 103554.

Bortolo, G.C., and F.C.T. Lima. 2020. A new species of *Cyphocharax* (Characiformes: Curimatidae) with a horizontal color pattern from the Rio Tapajós drainage, Amazon basin, Brazil. Neotropical Ichthyology 18 (2): e190135.

Bortolo, G.C., F.C.T. Lima, and B.F. Melo. 2018. A new *Cyphocharax* from the lower Rio Tapajós, Amazon basin, Brazil (Characiformes: Curimatidae). Copeia 106 (2): 346–352.

Castro, R.M.C., and R.P. Vari. 2004. Detritivores of the South American fish family Prochilodontidae (Teleostei: Ostariophysi; Characifomes). A phylogenetic and revisionary study. Smithsonian Contributions to Zoology 622: 1–189.

Dagosta, F.C., and M.C.C. de Pinna. 2019. The fishes of the Amazon: distribution and biogeographical patterns, with a comprehensive list of species. Bulletin of the American Museum of Natural History 431: 1–163.

Donohue, C.G., J.M. Hemmi, and J.L. Kelley. 2020. Countershading enhances camouflage by reducing prey contrast. Proceedings of the Royal Society of London B, Biological Sciences 287: 20200477.

Dutra, G.M., G. Vita, P.V. Gentile, L.E. Ochoa, and A.L. Netto-Ferreira. 2022. Integrative taxonomy reveals a new species of *Cyphocharax* (Characiformes: Curimatidae) from the Upper Paraíba do Sul River basin, Brazil. Neotropical Ichthyology 20 (3): e220017.

Edgar, R.C. 2004. MUSCLE: a multiple sequence alignment method with reduced time and space complexity. BMC Bioinformatics 5: 1–19.

Fowler, H.W. 1906. Further knowledge of some heterognathus fishes. Part I. Proceedings of the Academy of Natural Sciences, Philadelphia 58: 293–351.

Fricke, R., W.N. Eschmeyer, and R. Van der Laan. 2023. Eschmeyer's catalog of fishes: genera, species, references. Internet resource (http://researcharchive.calacademy.org/research/ichthyology/catalog/fishcatmain.asp), accessed April 6, 2023.

Hoorn, C., et al. 2010. Amazonia through time: Andean uplift, climate change, landscape evolution, and biodiversity. Science 330: 927–931.

Kearse, M., et al. 2012. Geneious Basic: An integrated and extendable desktop software platform for the organization and analysis of sequence data. Bioinformatics 28 (12): 1647–1649.

Kimura, M. 1980. A simple method for estimating evolutionary rates of base substitutions through comparative studies of nucleotide sequences. Journal of Molecular Evolution 16: 111–120.

Kumar, S., G. Stecher, M. Li, C. Knyaz, and K. Tamura. 2018. MEGA X: molecular evolutionary genetics analysis across computing platforms. Molecular Biology and Evolution 35: 1547–1549.

Maddison, W.P., and D.R. Maddison. 2021. Mesquite: a modular system for evolutionary analyses. Version 3.81. Internet resource (http://www.mesquiteproject.org), accessed April 6, 2023.

Mateussi, N.T.B., B.F. Melo, and C. Oliveira. 2020. Molecular delimitation and taxonomic revision of the wimple piranha *Catoprion* (Characiformes: Serrasalmidae) with the description of a new species. Journal of Fish Biology 97 (3): 668–685.

Melo, B.F. 2017. *Cyphocharax boiadeiro*, a new species from the upper Rio Araguaia, Amazon basin, Brazil (Characiformes: Curimatidae). Zootaxa 4247: 114–120.

Melo, B.F., and C. Oliveira. 2017. Three new species of *Curimatopsis* (Characiformes: Curimatidae) from the Amazon basin. Journal of Fish Biology 91 (2): 528–544.

Melo, B.F., and Vari, R.P. 2014. New species of *Cyphocharax* (Characiformes: Curimatidae) from the upper Rio Negro, Amazon basin. Neotropical Ichthyology 12 (2): 327–332.

Melo, B.F., R.C. Benine, T.C. Mariguela, and C. Oliveira. 2011. A new species of *Tetragonopterus* Cuvier, 1816 (Characiformes: Characidae: Tetragonopterinae) from the Rio Jari, Amapá, northern Brazil. Neotropical Ichthyology 9 (1): 49–56.

Melo, B.F., L.E. Ochoa, R.P. Vari, and Oliveira C. 2016. Cryptic species in the Neotropical fish genus *Curimatopsis* (Teleostei, Characiformes). Zoologica Scripta 45: 650–658.

Melo, B.F., et al. 2018. Molecular phylogenetics of Neotropical detritivorous fishes of the family Curimatidae (Teleostei: Characiformes). Molecular Phylogenetics and Evolution 127: 800–812.

Melo, B.F., J.S. Albert, F.C.P. Dagosta, and V.A. Tagliacollo. 2021. Biogeography of curimatid fishes reveals multiple lowland-upland river transitions and differential diversification in the Neotropics (Teleostei, Curimatidae). Ecology and Evolution 11: 15815–15832.

Melo, B.F., L.F.C. Tencatt, and C. Oliveira. 2022. Phylogenetic evidence for the *Cyphocharax saladensis* clade with description of a new species of *Cyphocharax* endemic to the upper Rio Paraguai Basin (Teleostei: Curimatidae). Ichthyology and Herpetology 110 (2): 327–339.

Netto-Ferreira, A.L., and R.P. Vari. 2011. New species of *Steindachnerina* (Characiformes: Curimatidae) from the Rio Tapajós, Brazil, and review of the genus in the Rio Tapajós and Rio Xingu basins. Copeia 2011 (4): 523–529.

Pattengale, N.D., M. Alipour, O.R. Bininda-Emonds, B.M. Moret, and A. Stamatakis. 2010. How many bootstrap replicates are necessary? Journal of Computational Biology 17 (3): 337–354.

Puillandre, N., S. Brouillet, and G. Achaz. 2021. ASAP: assemble species by automatic partitioning. Molecular Ecology Resources 21 (2): 609–620.Sabaj, M.H. 2022. Codes for natural history collections in ichthyology and herpetology, version 9.0 (14 February 2022). Internet resource (https://asih.org), accessed April 6, 2023.

Sidlauskas, B.L. and R.P. Vari. 2012. Diversity and distribution of anostomoid fishes (Teleostei: Characiformes) throughout the Guianas. Cybium 1: 71–103.

Stamatakis, A. 2014. RAxML version 8: A tool for phylogenetic analysis and post-analysis of large phylogenies. Bioinformatics 30 (9): 1312–1313.

Tamura, K., G. Stecher, and S. Kumar. 2021. MEGA11: molecular evolutionary genetics analysis version 11. Molecular Biology and Evolution 38 (7): 3022–3027.

Taylor, W.R., and G.C. Van Dyke. 1985. Revised procedures for staining and clearing small fishes and other vertebrates for bone and cartilage study. Cybium 9, 107–119.

Vari, R.P. 1984 Systematics of the Neotropical characiform genus *Potamorhina* (Pisces: Characiformes). Smithsonian Contributions to Zoology 400: 1–36.

Vari, R.P. 1989a. A phylogenetic study of the Neotropical characiform family Curimatidae (Pisces: Ostariophysi). Smithsonian Contributions to Zoology 471: 1–71.

Vari, R.P. 1989b. Systematics of the neotropical characiform genus *Curimata* Bosc (Pisces: Characiformes). Smithsonian Contributions to Zoology 474: 1–63.

Vari, R.P. 1989c. Systematics of the neotropical characiform genus *Psectrogaster* Eigenmann and Eigenmann (Pisces: Characiformes). Smithsonian Contributions to Zoology 481: 1–43.

Vari, R.P. 1989d. Systematics of the neotropical characiform genus *Pseudocurimata* Fernández-Yépez (Pisces: Ostariophysi). Smithsonian Contributions to Zoology 490: 1–26.

Vari, R.P. 1991. Systematics of the neotropical characiform genus *Steindachnerina* Fowler (Pisces, Ostariophysi). Smithsonian Contributions to Zoology 507: 1–118.

Vari, R.P. 1992a. Systematics of the Neotropical characiform genus *Cyphocharax* Fowler (Pisces, Ostariophysi). Smithsonian Contributions to Zoology 529: 1–137.

Vari, R.P. 1992b. Systematics of the neotropical characiform genus *Curimatella* Eigenmann and Eigenmann (Pisces, Ostariophysi), with summary comments on the Curimatidae. Smithsonian Contributions to Zoology 533: 1–48.

Vari, R.P. 2003. Family Curimatidae. *In* R.E. Reis, S.O. Kullander, and C.J. Ferraris Jr. (editors), Check list of the freshwater fishes of South and Central America: 51–64. Porto Alegre, Brazil: Edipucrs.

Vari, R.P., and T.A. Blackledge. 1996. New curimatid, *Cyphocharax laticlavius* (Ostariophysi: Characiformes), from Amazonian Ecuador, with a major range extension for *C. gouldingi*. Copeia 1996: 109–113.

Vari, R.P., and F. Chang. 2006. *Cyphocharax derhami*, a new species (Ostariophysi: Characiformes: Curimatidae) from northeastern Peru. Ichthyological Exploration of Freshwaters 17: 93–96.

Vari, R.P., A.M. Zanata, and P. Camelier. 2010. New species of *Cyphocharax* (Ostariophysi: Characiformes: Curimatidae) from the Rio de Contas Drainage, Bahia, Brazil. Copeia 2010: 382–387.

Vari, R.P., B.L. Sidlauskas, and P.Y. Le Bail. 2012. New species of *Cyphocharax* (Ostariophysi: Characiformes: Curimatidae) from Suriname and French Guiana and a discussion of curimatid diversity on the Guiana Shield. Cybium 36: 63–69.

Wosiacki, W.B., and D.P.S. Miranda. 2013. Description of a new small species of the genus *Cyphocharax* (Characiformes: Curimatidae) from the lower Amazon basin. Copeia 2013: 627–633.

Zhang, J., P. Kapli, P. Pavlidis, and A. Stamatakis. 2013. A general species delimitation method with applications to phylogenetic placements. Bioinformatics 29 (22): 2869–2876.

All issues of *Novitates* and *Bulletin* are available on the web (https://digitallibrary.amnh.org/handle/2246/5). Order printed copies on the web from:
https://shop.amnh.org/books/scientific-publications.html

or via standard mail from:
American Museum of Natural History—Scientific Publications
Central Park West at 79th Street
New York, NY 10024

♾ This paper meets the requirements of ANSI/NISO Z39.48-1992 (permanence of paper).